ELSEVIER

Polymer 43 (2002) 1207–1214

polymer

www.elsevier.com/locate/polymer

Synthesis, characterization, and properties of a novel acrylic terpolymer with pendant perfluoropolyether segments

Elena Casazza[a], Alberto Mariani[b], Laura Ricco[a], Saverio Russo[a,*]

[a]*Dipartimento di Chimica e Chimica Industriale, Università di Genova, via Dodecaneso 31, 16146 Genova, Italy*
[b]*Dipartimento di Chimica, Università di Sassari, via Vienna 2, 07100 Sassari, Italy*

Received 29 April 2001; accepted 2 November 2001

Abstract

A novel acrylic terpolymer with pendant perfluoropolyether (PFPE) segments has been synthesized and fully characterized. By hexamethylene diisocyanate functional groups PFPE monofunctional macromonomers have been grafted on a poly(butyl methacrylate-*co*-hydroxyethyl acrylate-*co*-ethyl acrylate) random terpolymer. Such grafted copolymer behaves like an interface-active material, since the perfluoropolyether segments in solvent cast films rearrange themselves at the air–polymer interface by surface segregation. In addition, blends of the above graft copolymer with acrylic base polymers (either the terpolymer itself or a commercial copolymer) have been examined in terms of surface segregation and fluorine enrichment of the external layers.

The critical surface tension, γ_c, of solid films made of the neat graft copolymer as well as of the polymer blend has been evaluated by contact angle measurements and Zisman plots. Even a small addition (5 wt%) of the fluorinated copolymer to the acrylic component has been found very effective in lowering the surface tension. The outermost surface composition has been investigated by XPS technique, confirming the strong fluorine enrichment. Furthermore, SEM and EDX analyses have been performed on cross-sectioned films, showing that in the above polymer blends macrophase surface segregation has originated a thick layer made of fluorinated copolymer close to the air–polymer interface.

Keywords: Perfluoropolyether; Graft copolymer; Surface segregation

1. Introduction

In the last few decades many polymers, such as polyacrylics, polyurethanes, epoxy resins, polysiloxanes, fluoropolymers, etc. have been largely employed as protective materials primarily in the conservation of stone monuments and historical buildings, providing a thin cover layer more or less regularly distributed on their surface. In general, the durability of the above protective agents has unfortunately shown to be rather short, due to their limited resistance toward atmospheric factors (UV radiation, temperature fluctuations, pollution, etc.) [1–3]. As an exception, fluorinated polymers [4–6] have proved to be the best among protective materials because of both their higher stability (due to the relevant strength of carbon–fluorine bond) and the hydrophobic characteristics. Indeed, surface hydrophobicity is the most relevant prerequisite for an effective stone protection, since polluted atmospheric water is a very detrimental and harmful agent in any respect [7].

Among fluorinated polymers, perfluoropolyethers (PFPE) seem to exhibit the most suitable properties as protective agents [8–10]. PFPEs [11], besides being transparent, odorless, and tasteless fluids possess high thermal, oxidative, and hydrolytic stability. Moreover, they are chemically inert to the majority of reagents including mineral and organic acids and bases, oxidizing and reducing agents and halogens. They are characterized by the lowest CED values ever found for all classes of compounds, even lower than that of poly(tetrafluoroethylene) (PTFE), and exhibit extremely low surface tension (12–20 dynes/cm) [11].

However, PFPEs show two drawbacks that severely limit their utilization in the ancient stone preservation field: the first refers to their very high cost, the second is related to their strong tendency to migrate away from the stone substrate according to both their oily consistency and the low adhesion properties. Therefore, our aim has been not only to reduce PFPE content in the protective agent formulation, but also to improve its anchoring to the substrate by binding the PFPE segments to an acrylic polymer having good adhesion properties, synthesized on-purpose. To achieve a further cost abatement, we have made blends of

* Corresponding author. Tel.: +39-010-353-6198; fax: +39-010-353-6199.
E-mail address: russo@chimica.unige.it (S. Russo).

0032-3861/02/$ - see front matter
PII: S0032-3861(01)00722-4

our partially fluorinated copolymer with the unmodified acrylic polymer, as well as with a commercial protective agent (Paraloid B72®, Rohm and Haas), taking advantage of the well-known phenomenon of surface segregation [12,13], able to push the fluorinated segments on the outer surface. Indeed, when small amounts of fluorinated oligomers/polymers are mixed to various polymers, the former ones are very effective in lowering the surface free energy of the latter due to extensive fluorine enrichment of the surface [14–16]. On this basis, also in order to circumvent difficulties and costs associated with producing new fluoropolymers for different applications, fluorine-containing additives have been used in the past to modify surface properties of conventional hydrocarbon polymers. Unfortunately, the very poor compatibility of fluorocarbon additives with the conventional polymers reduces the usefulness of such approach. Therefore, it seemed to us more convenient to covalently link fluorinated segments to a suitable hydrocarbon polymer, thus obtaining a heterophase copolymer similar in behavior to the block or graft copolymers described in the literature [17]. In fact, polymers with highly fluorinated side chains linked to a sequence of the block copolymer act as surface-active polymers [18]. Near the surface, the block copolymer shows strong segregation due to the lower surface free energy component [19,20]. Segregation is driven by both the unfavorable enthalpy interactions and the decrease of the bare surface free energy, caused by replacing the base polymer segments of higher surface free energy with low surface free energy block segments.

As is well known, at a given bulk composition the extent of surface segregation depends on the specific type of polymer system to deal with [21], e.g. a neat block copolymer, a blend of homopolymers, a copolymer/homopolymer blend, or a blend of copolymers. Namely, the morphology of block copolymer surfaces widely differs from that of the corresponding homopolymer blends, inasmuch as in copolymers the constituents are obviously interconnected and cannot undergo macrophase separation as polymer blends do. Therefore, near the outer surface, copolymers are known to form spatially periodic phases on molecular size scale, similar to those found in bulk (spheres, lamellas, cylinders, more complex morphologies) [22,23]. Studies carried out by both XPS and angular dependent XPS on surface composition of a linear multiblock copolymer, in which one block is constituted of PFPE sequences, have clearly shown that the fluorinated segments are located near the polymer–air interface and that there is an optimum PFPE MW for phase segregation [24]. However, unlike polymer blends, the composition profile in the close-to-surface region of a diblock copolymer generally exhibits oscillations [22] because of the connectivity of the segments. On the contrary, the equilibrium surface volume fraction of a miscible homopolymer blend is simply a function of the following parameters: bulk volume fraction, difference of surface free energy between the two components, degree of polymerization, polymer architecture and Flory–Huggins interaction parameter χ. Because of the very small entropy of mixing for a polymer blend, the formation of an enriched layer costs very little in terms of free energy; thus a small difference in surface free energy is sufficient to generate a remarkable segregation. As a consequence, the entity of the surface enrichment is mainly determined by the bulk thermodynamics, e.g. the value of χ parameter [25]. In an immiscible binary blend (e.g. fluorinated polymer/hydrogenated polymer), since equilibrium bulk thermodynamics favors complete demixing of the two components, the 'equilibrium' surface should be exclusively occupied by the constituent of lower surface free energy [26–28]. Thus, a fluorine enriched surface can be prepared either introducing perfluorinated chains in a hydrocarbon polymer (e.g. polyacrylates having fluorocarbon pendant groups [13,16,29]) or blending hydrocarbon polymers with fluorine containing polymers [30–32].

2. Experimental

2.1. Materials

n-Butyl methacrylate (BMA) and ethyl acrylate (EA) monomers (Aldrich) were purified by percolation through an inhibitor-removal column (Aldrich). 2-Hydroxyethyl acrylate monomer (HEA), inhibitor free (Aldrich), was purified from diacrylate by hexane extraction of the 25% v/v monomer/water solution; acrylic acid was then removed by ether extraction.

The isocyanate-monofunctionalized PFPE (CF_3O–$(C_3F_6O)_m$–$(CF_2O)_n$–CF_2CH_2–$OCONH(CH_2)_6NCO$) (PFPE–HMDI), derived from the condensation between a hydroxyl terminated perfluoropolyether (Fomblin Y) and hexamethylene diisocyanate (HMDI) was kindly supplied by Dr C. Tonelli, Ausimont S.p.A. (equivalent weight (from ^{19}F-NMR) = 872; (from end group titration) = 1015; MW (from ^{19}F-NMR) = 935 g/mol, MW (from end group titration) = 1064 g/mol. Bifunctional PFPE = 7.17%. FT-IR (NaCl): 3350m, 2940m, 2864w, 2277s, 1732s, 1526m, 1240vs, 1144s, 983m (cm^{-1}). ^{1}H-NMR($CDCl_3$): δ 1.36 and δ 1.57 (8H, 2m), δ 3.18 and δ 3.29 (4H, 2 m), δ 4.42 (2H, t), δ 4.88 (1H, t). T_g(20 °C/min) = −70 °C.

2.1.1. Synthesis of poly(butyl methacrylate-co-hydroxyethyl acrylate-co-ethyl acrylate), P(BMA-HEA-EA)

The random terpolymer was prepared by radical solution polymerization in THF at 50 °C for 90 min, using AIBN as initiator (1 wt% based on the total monomer content). The monomers (66.6 mol% BMA, 20.4 mol% HEA, 13.0 mol% EA) were dissolved in THF in the ratio 1:3 (v/v). The resulting polymer was recovered by dropwise precipitation in petroleum ether at 0 °C and purified twice by dissolution–precipitation cycles. The purified terpolymer was dried in a vacuum oven at 50 °C for 24 h and then kept in a desiccator.

FT-IR (neat): 3550w, 2960m, 2936m, 2874w, 1730vs, 1466m, 1386w, 1241s, 1157s. ^{1}H-NMR ($CDCl_3$): δ 0.94(t), δ 1.25(t), δ 1.39(m), δ 1.59(m), δ 1.85(m), δ 3.78(m), δ 3.94(m). Intrinsic viscosity (chloroform, 20 °C) = 0.70 dl/g. T_g(20 °C/min) = 19 °C. Molecular weight from GPC determination: M_n = 96 000, M(peak) = 135 000, M_w = 164 000 g/mol, polydispersity = 1.71 (based on PMMA standards).

2.1.2. Synthesis of poly(BMA-HEA-EA)-g-(PFPE-HMDI)

The random terpolymer poly(BMA-HEA-EA) was dissolved in anhydrous THF (3% wt/v) under overnight stirring in nitrogen atmosphere. An equimolar amount of PFPE–HMDI was then added. Dibutyltin dilaurate (DBTDL) was used as catalyst (1 wt% based on PFPE–HMDI). The reaction was carried out at 60 °C for 8 h under reflux. The solution was then precipitated in petroleum ether at 0 °C. The graft copolymer was purified by dissolving it in THF and reprecipitation in petroleum ether. FT-IR (neat): 3350w, 2960m, 2936m, 1533w, 1386w, 2874m, 1730vs, 1466w, 1256s, 1140s, 983w. ^{1}H-NMR ($CDCl_3$): δ 0.94(t), δ 1.38(m), δ 1.58(m), δ 3.18(m), δ 3.94(m), δ 4.25, δ 4.42(t). Intrinsic viscosity (chloroform, 20 °C) = 0.80 dl/g. $T_{g(1)}$(20 °C/min) = −70 °C, $T_{g(2)}$ = 20 °C.

2.2. Characterization and properties

2.2.1. Film preparation

Films of neat graft polymers as well as of their blends with the parent terpolymer or Paraloid® were prepared by casting from 2% (wt/v) THF solutions on PTFE or PP Petri dishes. In particular, the blend solutions were prepared by mixing suitable amounts of the polymeric components under stirring (5 h). All film samples were dried in air for a week.

2.2.2. Contact angle measurement

Contact angles of three series of testing liquids were measured with an optical Krüss goniometer, model G 23. The 1.5–2.0 mm diameter drops of liquids, dripped from a microsyringe, were put on the film surface at 20 °C. The wetting liquids were distinguished by their polarity in D, P, and H liquids. The surface tensions γ_L of the organic liquids, divided in their dispersion (D), polar (P) and hydrogen bonding contributions (H) [33–35], are summarized in Table 1.

Table 1
Surface tensions of liquids at 20 °C (in dynes/cm) [33]

Type	Liquid	γ_L^D	γ_L^P	γ_L^H	γ_L
D	*n*-Octane	21.8	0	0	21.8
	n-Nonane	22.9	0	0	22.9
	n-Decane	23.9	0	0	23.9
	n-Undecane	24.7	0	0	24.7
	n-Dodecane	25.4	0	0	25.4
	n-Tetradecane	26.7	0	0	26.7
	n-Esadecane	27.6	0	0	27.6
P	1,1,2 Trichloroethane	–	–	–	33.6
	Tetrachloroethane	33.2	3.1	0	36.3
	1,2 Dibromoethane	–	–	–	38.9
	α-Bromonaphthalene	44.4	0.2	0	44.6
	Tetrabromoethane	44.3	3.2	0	47.5
H	Methanol[a]	29.4	–	–	22.6
	Dipropylenglycol	29.9	0	4.5	33.9
	Polyethylenglycol	31.7	0.1	13.5	43.5
	Diethylenglycol	–	0	12.7	44.4
	1,4 Butanediol[a]	30.1	–	–	45.2
	Ethylene glycol		0	17.6	47.7

[a] Data from Ref. [35].

2.2.3. Instrumentation

Transmission infrared spectra were obtained on neat polymer films by a Bruker FT-IR spectrometer, model FIS 66. ^{1}H-NMR spectra of $CDCl_3$ solutions were recorded by a Gemini 200 MHz Varian spectrometer. A Mettler DSC 30 equipped with a Mettler TC 10A processor monitored thermal transitions. Glass transition temperatures were obtained from the curves recorded at 20 °C/min as the midpoints of the step variation in the third run. SEM micrographs of the film cross sections were performed on a Leo Stereoscan 440 electron microscope and the EDS (EDX) analysis carried out by an Oxford Link Gem analyzer. The film sections were sliced normal to the film surface and carbon or aluminum coated. Care was taken to limit the electron radiation damage on the polymer sample surface during EDS analysis.

The XPS measurements were performed on the air-exposed surface by a Physical Electronics PHI 5600 ESCA system, using an Al mono $K\alpha_{1,2}$ X-ray source (1256.6 eV). The X-ray source was working at 350 W and 117.4 eV.

The GPC characterization was carried out using a Waters 2690 separation module equipped with a 2410 Differential Refractive Index Detector. The column set was constituted of four styrene-divinylbenzene Ultrastyragel columns (Waters) (30 cm L., 7.8 mm I.D., 10 μm particle size, 500 + 10^3 + 10^4 + 10^5 Å pore size). The solvent was HPLC grade chloroform stabilized with amylenes (Aldrich) (solution concentration 0.2% (w/v); injection volume 100 μl; flow rate 1.0 ml/min; column temperature 35 °C). The relative calibration curve was calculated with poly (methylmethacrylate) (PMMA) narrow standards (Aldrich) with MW from 2500 up to 800 000 g/mol.

3. Results and discussion

3.1. Graft copolymer and its blends

We have synthesized a novel partially fluorinated graft polymer constituted of a polyacrylic backbone (random terpolymer formed by BMA, HEA and EA units) and

perfluoropolyether side chains. The PFPE segment, derived from the NCO-monofunctionalized perfluoropolyether (PFPE–HMDI), was linked to the acrylic backbone by an urethane bond formed by the reaction of the –NCO functional group with the –OH group of HEA. As mentioned in Section 1, it can be assumed that the graft polymer should behave as an interface-active material and that the PFPE segments at lower surface free energy should rearrange themselves in the close-to-air region. In other words, the fluorinated side chains would almost entirely cover the surface layer of the graft polymer film. As quoted above, suitable blending of the fluorine-containing graft polymer with a hydrocarbon base polymer (e.g. the parent acrylic terpolymer) would favor the additional migration of the fluorine-containing component to the surface region [31,32], where it is driven by the lower free energy PFPE side chains. Thus, the fluorinated chains are expected to stay in the outermost region (on a nanometric scale) [13,22,36].

To verify the above expectations, as stated in Section 2, the PFPE-containing graft copolymer and the acrylic base resins (either the terpolymer or a commercial product) have been blended together at various weight ratios (5, 10 and 20%) and the resultant blends investigated as solid films by SEM, EDS (EDX) and XPS techniques. On the same blends, critical surface tensions [34] following Zisman [37] have been determined by contact angle measurements using the testing liquids listed in Table 1.

3.2. Product characterization

The ^{1}H-NMR spectra represented in Fig. 1 refer to (a) PFPE–HMDI, (b) the acrylic terpolymer, and (c) the product after grafting. It is evident that the peak at 3.8 ppm, assigned to the $-CH_2-$ adjacent to the hydroxyl group (Fig. 1b), is completely absent in the grafted copolymer (Fig. 1c), where the peak of the same $-CH_2$, now adjacent to the –OCONH– group, appears at 4.1 ppm. In the spectrum of the fluorinated graft copolymer, two more peaks are visible at 3.15 and 4.1 ppm; they are relative to the central $-CH_2-$ groups in the hexamethylene segment (from HMDI) and to the $-CH_2$ adjacent to the CF_2 group in PFPE, respectively. In addition, the FT-IR spectra confirm that all –OH groups in P(BMA-HEA-EA) have reacted with the terminal –NCO group of (PFPE–HMDI).

3.3. Critical surface tensions

As mentioned above, the critical surface tensions γ_c have been determined for blends in which the fluorinated graft copolymer was mixed (at the concentration of 5, 10, 20% by weight) either with the parent terpolymer P(BMA-HEA-EA) or with the commercial copolymer Paraloid B72, i.e. poly(ethylmethacrylate-*co*-methylacrylate). In order to obtain the reference values of this parameter, analogous measurements were performed on the neat copolymer films. The γ_c values have been estimated by extrapolating the straight lines corresponding to homogeneous liquids (the

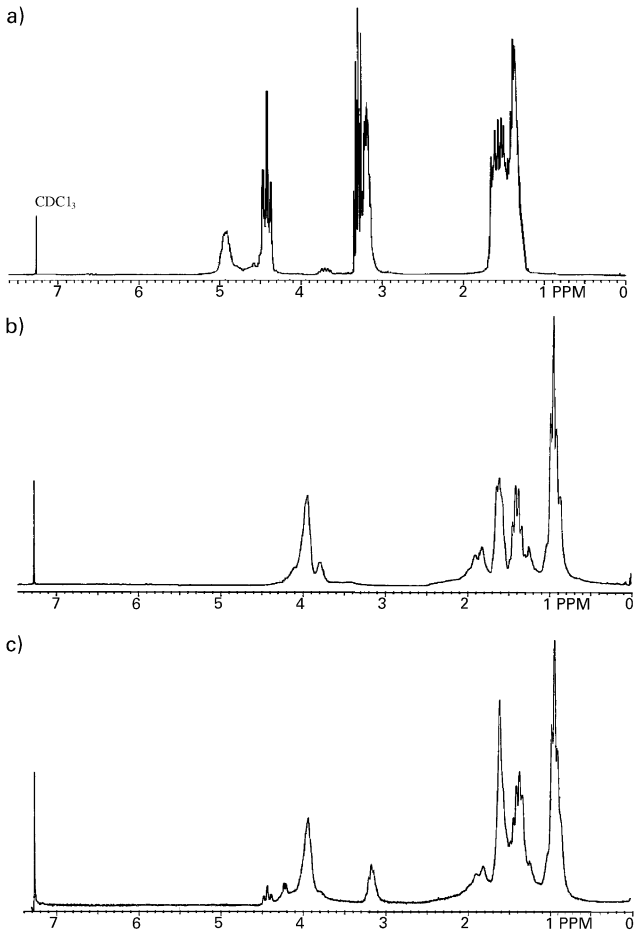

Fig. 1. ^{1}H-NMR spectra of: (a) PFPE–HMDI, (b) P(BMA-HEA-EA), (c) P(BMA-HEA-EA)-*g*-(PFPE-HMDI).

D, H and P species, respectively, listed in Table 1) in the cos θ vs. γ_L plots (Figs. 2–4 as examples). The results for the neat copolymers and for the copolymer blends are summarized in Tables 2 and 3, respectively. The γ_c values referred to the (P) liquids are notably larger than those obtained with the (H) and (D) ones, while the values of the latter ones do not significantly differ from each other.

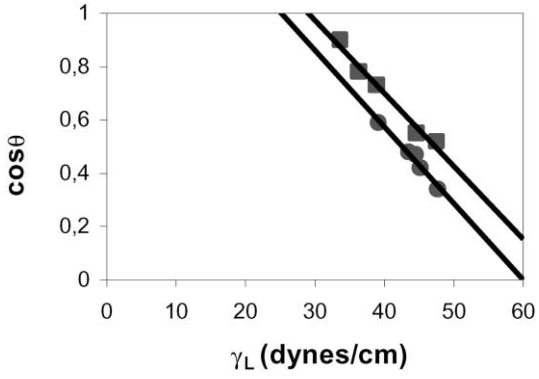

Fig. 2. The cos θ *vs.* γ_L plot of the P(BMA-HEA-EA) (EC6). (●) H-liquids; (■) P-liquids.

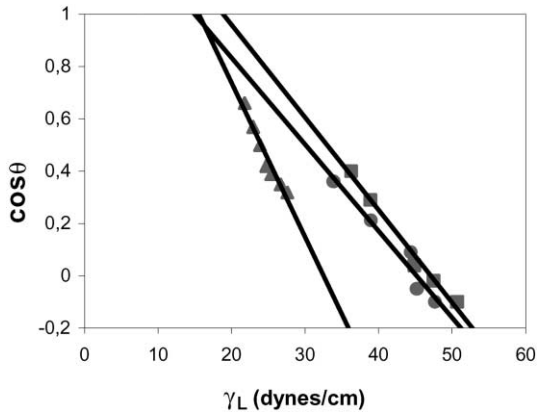

Fig. 3. The cos θ vs. γ_L plot of P(BMA-HEA-EA)-g-(PFPE-HMDI) (EC6-F). (▲) D-liquids; (●) H-liquids; (■) P-liquids.

Obviously, (P) liquids may show strong interactions with polymer films (swelling, dissolution, etc.), greatly affecting the 'apparent' values of surface tensions. In the present study, we cannot analyze this behavior in depth. However, it is well known that, in general, the γ_c values vary according to the kind of liquids used, e.g. dispersion, polar, or hydrogen bonding liquids [34]. It has been found from our measurements that even small additions (5–10%) of the graft copolymers to the acrylic base polymer have a great effect on reducing the surface tension of the polymer film, with γ_c that approaches the value found for the neat fluorinated copolymer (15–16 dynes/cm with (D) liquids). Increasing the bulk concentration up to 20% does not affect the γ_c values significantly; consequently, it can be safely argued that the surface composition is not appreciably changed. These results show that 5% concentration of the grafted polymer is more than enough to generate a topmost layer predominantly constituted of the fluorinated segments.

3.4. SEM and EDX analysis

The cross-sectioned films of the P(BMA-HEA-EA)-*g*-(PFPE-HMDI)/P(BMA-HEA-EA) blends (with weight ratios of 5/95, 10/90 and 20/80) were investigated by scanning electron microscopy and by energy dispersive X-ray spectroscopy in order to evaluate the surface segregation and the fluorine concentration (in terms of F/C ratios). The SEM micrographs show a sharp accumulation of fluorinated materials close to the air–polymer interface. In the (20/80) blend (Fig. 5), the presence of a thick layer of the fluorine containing copolymers (in clearer gray) is easily visible at the left side of the section relative to the air–polymer interface. The fluorine concentration detected by EDX analysis confirms the strong presence of such fluorinated layer (see the fluorine mapping in Fig. 6). Relevant accumulation of fluorinated segments is also evident at the opposite side, corresponding to the film surface that has been in contact with the PTFE capsule during solvent evaporation. The relatively high specific weight of the PFPE-containing polymer, combined with its strong affinity with PTFE, contributes to favor its deposition also on the

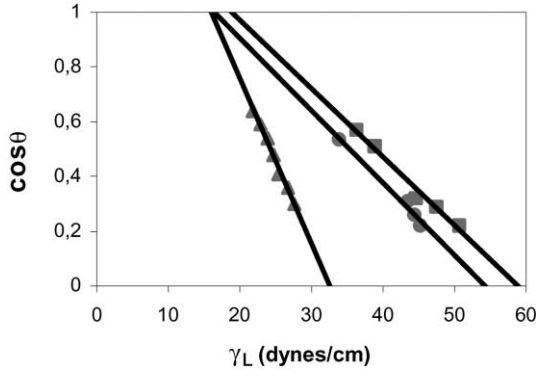

Fig. 4. The cos θ *vs.* γ_L plot of P(BMA-HEA-EA)-*g*-(PFPE-HMDI)/P(BMA-HEA-EA) (10/90) blend (EC6-F/EC6). (▲) D-liquids; (●) H-liquids; (■) P-liquids.

Table 2
Critical surface tensions of the acrylic base terpolymers and PFPE-grafted polymers

Sample name	Polymer	γ_c	
		(dynes/cm)	Liquid type
B 72	P(EMA-MA)	30.5	H
EC5	P(BMA-HEA-EA)	25.1	H
		28.6	P
EC6	P(BMA-HEA-EA)	25.2	H
		29.1	P
		15.8	D
EC5-F	P(BMA-HEA-EA)-*g*-(PFPE-HMDI)	15.2	H
		19.1	P
		15.5	D
EC6-F	P(BMA-HEA-EA-)*g*-(PFPE-HMDI)	14.9	H
		18.9	P

Table 3
Critical surface tensions of the polymer blends

Composition of the blend (weight ratio)	γ_c (dynes/cm)	Liquid species
EC5-F/Paraloid B72 (5/95)	17.0	D
EC5-F/Paraloid B72 (10/90)	14.9	D
	15.8	H
	16.7	P
EC6-F/Paraloid B72 (10/90)	14.8	D
EC5-F/EC5 (5/95)	17.1	D
EC5-F/EC5 (10/90)	16.5	D
	20.2	P
EC5-F/EC5 (20/80)	15.6	D
	15.0	H
	19.1	P
EC6-F/EC6 (5/95)	17.2	D
EC6-F/EC6 (10/90)	16.0	D
	16.4	H
	18.8	P

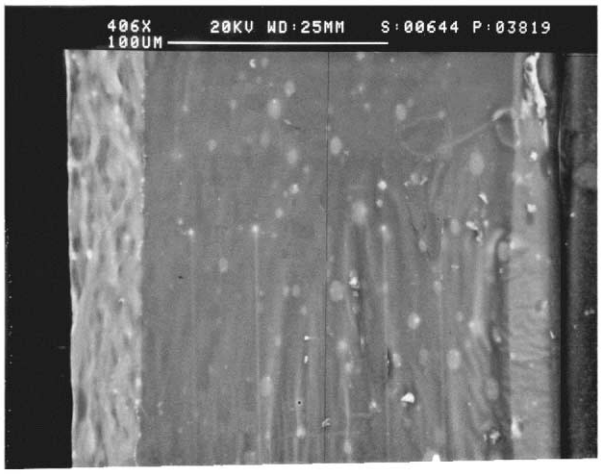

Fig. 5. SEM micrograph of the film section across the (BMA-HEA-EA)-*g*-(PFPE-HMDI)/(BMA-HEA-EA) (20/80) blend. The fluorinated material is represented by the clearer gray areas.

bottom of the Petri dish. This typical behavior has been found even in the (10/90) and (5/95) blends (see histograms of Fig. 7). The predominant migration of relevant amounts of the fluorinated graft polymer to the film–air interface yields a high fluorine concentration in the topmost regions (0–20 μm (Fig. 7). The 5/95, 10/90 and 20/80 blends exhibit, in the 0–20 μm region, a F/C ratio equal to 54.4, 69.4, and 79.8%, respectively (having a bulk F/C value of about 1–5%). Because of the remarkable immiscibility between the acrylic backbone and the PFPE sequences in the graft copolymer, macrophase separation may already occur in bulk, originating micelles of various shapes and dimensions. This phenomenon is particularly evident in the (20/80) blend, where phase inversions are also visible: fluorinated micelles separate inside the acrylic phase and acrylic micelles separate into the segregated fluorinated layer (Fig. 8).

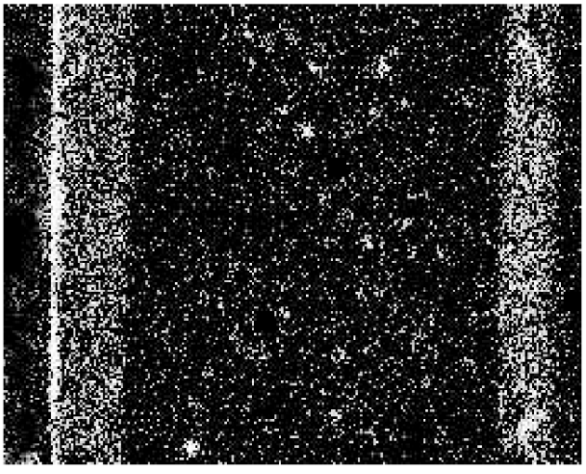

Fig. 6. The EDX mapping of the fluorine presence in the film section across the P(BMA-HEA-EA)-*g*-(PFPE-HMDI)/P(BMA-HEA-EA) (20/80) blend. The film has been solvent cast on PTFE dishes.

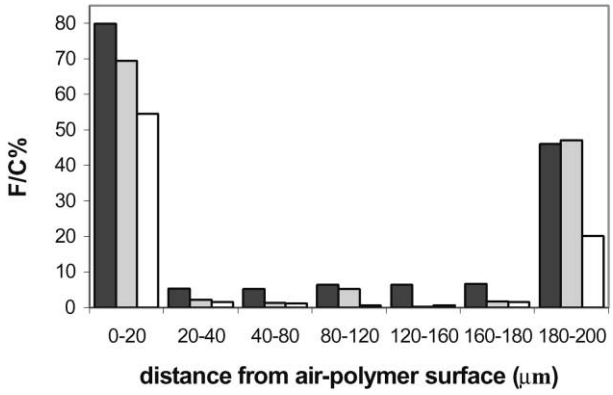

Fig. 7. The fluorine concentration, detected by EDX analysis, in the film sections across the P(BMA-HEA-EA)-*g*-(PFPE-HMDI)/P(BMA-HEA-EA) blends: (■) (20/80); (▒) (10/90); (□) (5/95).

3.5. XPS analysis

The film surfaces relative both to the graft polymer P(BMA-HEA-EA)-*g*-(PFPE-HMDI) and to the P(BMA-HEA-EA)-*g*-(PFPE-HMDI)/P(BMA-HEA-EA) (5/95) blend have been investigated by X-ray photoelectron spectroscopy in order to evaluate the surface fluorine concentration (Fig. 9). The detected area was ca. 400 μm and the sampling depth 2–6 nm (the PFPE side chain is less than 2 nm long and the HMDI-PFPE sequence is ca. 4 nm). The graft copolymer film shows a surface atomic composition of 39.6% F, 39.9% C, 14% O, 4.4% N (Fig. 9). Since the fluorine content is approximately 10% in the graft copolymer, 50–55% in the PFPE–HMDI sequences, and 60–65% in the PFPE portion of the latter, respectively, also these data suggest that the fluorinated side chains predominantly move to the air–polymer interface. The fluorine content present there, however, is lower than the theoretical value

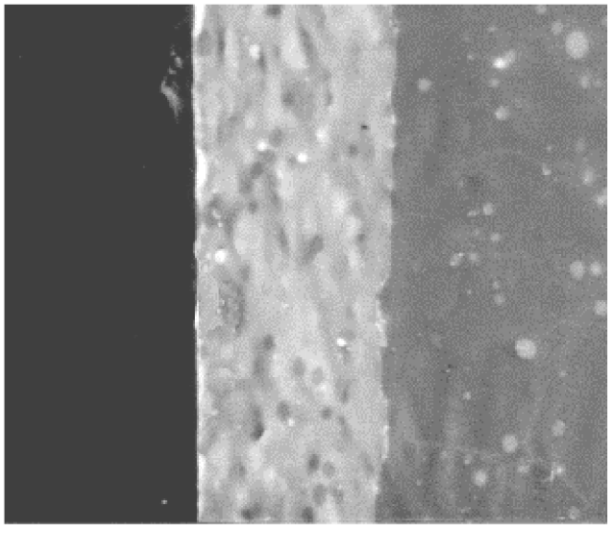

Fig. 8. The fluorinated surface layer (in clearer gray) in the cross-sectioned film relative to (BMA-HEA-EA)-*g*-(PFPE-HMDI)/(BMA-HEA-EA) (20/80). The phase separation in micelles is also visible.

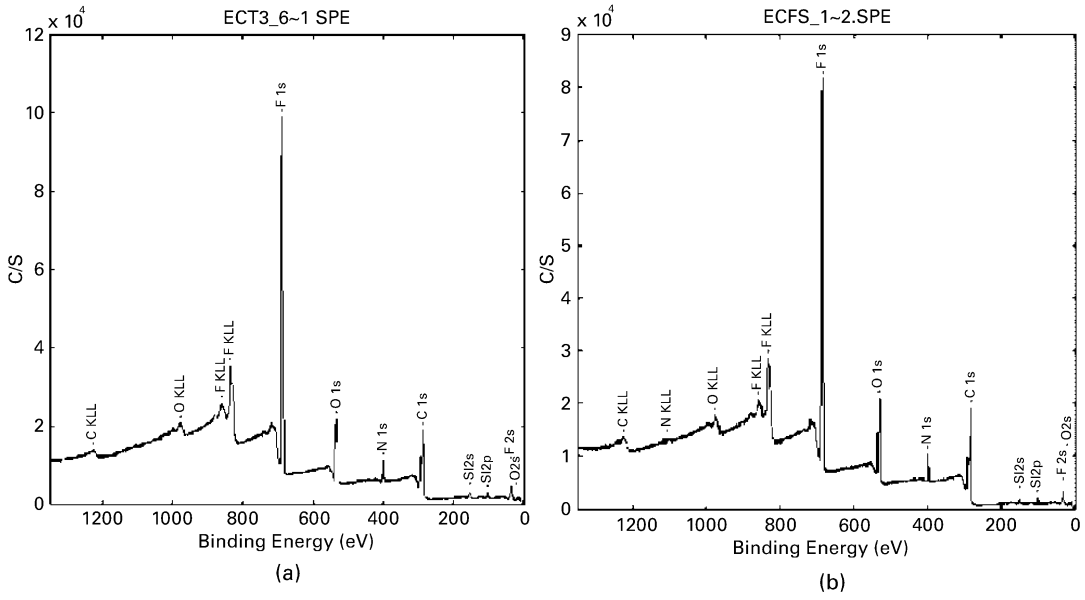

Fig. 9. XPS spectra of: (a) the neat P(BMA-HEA-EA)-*g*-(PFPE-HMDI), (b) the P(BMA-HEA-EA)-*g*-(PFPE-HMDI)/P(BMA-HEA-EA) (5/95) blend.

of about 50–55% which would correspond to a surface layer constituted only of PFPE–HMDI segments. Indeed, this is simply an artifact due to the sampling depth in our XPS analysis, greater than the PFPE–HMDI length.

The (5/95) blend surface exhibits values of 35.8% F, 42.5% C, 15% O, 5.2% N (Fig. 10). The surface enrichment in the blend, in terms of fluorine (for which the overall bulk F content is 0.5–1%), is close to that found in the neat graft polymer.

All results suggest that a little amount of P(BMA-HEA-EA)-*g*-(PFPE-HMDI) (about 5 wt%), blended with the acrylic terpolymer, is indeed sufficient to create a surface layer enriched in fluorine, i.e. with the PFPE–HMDI side chains located in the outermost region, similarly to the behavior of neat fluorinated copolymer. Recently, very relevant surface enrichment of fluorine-containing segments has been found by Bongiovanni et al. [13] in a MMA copolymer containing PFPE side groups ($T_{g(1)} = -120$ °C ca., $T_{g(2)} = 113$ °C ca.)

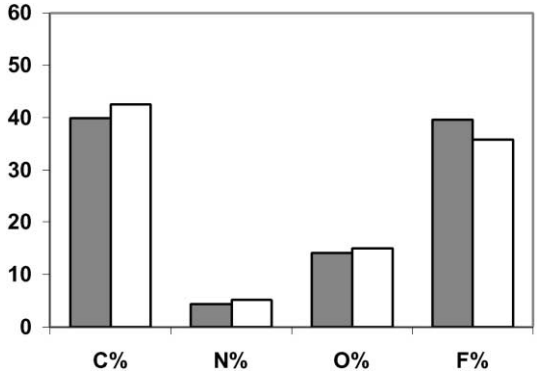

Fig. 10. XPS surface composition: (■) neat P(BMA-HEA-EA)-*g*-(PFPE-HMDI); (□) P(BMA-HEA-EA)-*g*-(PFPE-HMDI)/P(BMA-HEA-EA) (5/95) blend.

4. Conclusions

We have found a strong macrophase surface segregation of P(BMA-HEA-EA)-*g*-(PFPE-HMDI) when added to the base P(BMA-HEA-EA). This segregation gives rise to a relatively thick fluorinated surface layer mainly constituted of the acrylic-*g*-PFPE copolymer. Moreover, this surface coating approaches the surface composition of the neat P(BMA-HEA-EA)-*g*-(PFPE-HMD) polymer, in which the PFPE side chains stay in the outermost region, providing good characteristics of hydrophobicity and stability. We have proved that the segregated fluorinated polymer covering the surface of the blend confers the same surface properties found for the neat graft copolymer film. These results suggest that P(BMA-HEA-EA)-*g*-(PFPE-HMDI) copolymer is an excellent protective material [38] (e.g. for stone monuments), the same must be true for its blends, despite the very small PFPE bulk concentration. The fluorinated coating, originated by surface segregation, might be sufficient to guarantee stone protection from atmospheric agents, with a much lower cost as compared to PFPE-based materials. Moreover, its grafting and subsequent blending favor the stable anchoring of protective formulations to the stone itself.

Acknowledgements

The authors express their thanks to Ausimont S.p.A. (Dr C. Tonelli) for supplying PFPE-HMDI, Drs R. Parodi and A. Daccà (Department of Physics, University of Genoa) for

XPS characterization and Mr C. Uliana for the SEM, EDX analysis. PF 'Beni Culturali' funds are gratefully acknowledged.

References

[1] Hawkins WL. Conservation of historic stone buildings and monuments. Washington, DC: National Academic Press, 1982. p. 322.
[2] Rånby B, Rabeck JF. ACS Symposium. Washington: American Chemical Society, 1983. p. 229.
[3] Charola AE, Laurenzi Tabasso M, Santamaria U. Determination and Conservation of Stone. In: Preprint of the Vth International Congress. Lausanne, 1985. p. 739.
[4] Matteoli U, Aglietto M, Fassina V, Botteghi C, Passaglia E, Ciardelli F. Methods of Evaluating Products for the Conservation of Porous Building Materials in Monuments. In: Proceedings of the International Colloquium. Rome, 1995. p. 373.
[5] Tiano P, Manganelli Del Fa C, Fratini F, Pecchioni E, Lucido V, Piacenti F. Determination and Conservation of Stone. In: Proceedings of the VIth International Congress. Torun, 1988. p. 492.
[6] Piacenti F, Camaiti M, Manganelli Del Fa C, Scala A. Conservation of Stone and Other Materials. In: Proceedings of the International RILEM/UNESCO Congress. Paris: E and FN Spon ed., 1993. p. 740.
[7] Lazzarini L, Laurenzi Tabasso M. Il Restauro della Pietra, Padova: Cedam ed., 1986.
[8] Moggi G. Adv Org Coat Sci Technol Ser 1991;13:3.
[9] Piacenti F. Sci Total Environ 1994;143:113.
[10] Moropoulou T, Theoulakis P, Dogas T. Science and Technology for Cultural Heritage 1994;3:113.
[11] Marchionni G, Ajroldi G, Pezzin G. In: Aggarwal SC, Russo S, editors. Comprehensive polymer science. Oxford: Pergamon Press, 1996. Second supplement.
[12] Wu S. In: Paul DR, Newman S, editors. Polymer blends, Vol. 1. New York: Academic Press, 1978.
[13] Bongiovanni R, Malucelli G, Lombardi V, Priola A, Siracusa V, Tonelli C, Di Meo A. Polymer 2000;42:2299 and references quoted therein.
[14] Chujo Y, Hiraiwa A, Kabayashi H, Yamashita Y. J Polym Sci 1988;26:2991.
[15] Park J, Lee SB, Choi CK. J Appl Polym Sci 1994;54:1449.
[16] Park IJ, Lee S-B, Choi CK. Macromolecules 1998;31:7555.
[17] Hunt Jr M, Belu AM, Linton RW, De Simone JM. Macromolecules 1993;26:4854.
[18] Iyengar DR, Perutz SM, Dai C-A, Ober CK, Kramer EJ. Macromolecules 1996;29:1229.
[19] Chen X, Gardella Jr JA, Ho T, Wynne KJ. Macromolecules 1995;28:1635.
[20] Catano Y, Tomono H, Nakajima T. Macromolecules 1994;27:2342.
[21] Pertsin AJ, Gorelova MM, Levin VY, Makarova LI. J Appl Polym Sci 1992;45:1195.
[22] Chen X, Gardella Jr J, Kumler PL. Macromolecules 1993;26:3778.
[23] Janert PK, Schick M. Macromolecules 1998;31:1109.
[24] Bottino F, Di Pasquale G, Pollicino A, Pilati F, Toselli M, Tonelli C. Macromolecules 1998;31:7814.
[25] Jones R, Kramer E. Polymer 1993;34:115.
[26] Affrossman S, Bertrand P, Hartshone M, Kiff T, Leonard D, Pethrick RA, Richards RW. Macromolecules 1996;29:5432.
[27] Bhatia QS, Pan DH, Koberstein JT. Macromolecules 1988;21:2166.
[28] Chen X, Gardella Jr JA. Macromolecules 1994;27:3363.
[29] Thomas RR, Anton DR, Graham WF, Darmon MJ, Sauer BB, Stika KM, Swartzfager DG. Macromolecules 1997;30:2883.
[30] Yuan Y, Shoichet MS. Macromolecules 2000;33:4926.
[31] Kano Y, Akiyama S, Kasemura T, Kobayashi S. Polym J 1995;27:339.
[32] Kano Y, Akiyama S. Polymer 1996;37:4497.
[33] Kano Y, Akiyama S. Polymer 1992;33:1690.
[34] Wu S. Polymer interfaces and adhesion. New York: M. Dekker, 1982.
[35] Handbook of Chemistry and Physics. 60th ed. Boca Raton, FL: CRC Press, 1980.
[36] Chapman TM, Benrashid R, Marra KG, Keener JP. Macromolecules 1995;28:331.
[37] Zisman WA. In: Fowkes FW, editor. Contact angle, wettability and adhesion, Vol. 43. Washington, DC: ACS Symposium Series, 1964.
[38] Camaiti M, Piacenti F, Casazza E, Ricco L, Russo S. (in preparation).